Neutrophils as sources of dinucleotide polyphosphates and metabolism by epithelial ENPP1 to influence barrier function via adenosine signaling

Valerie F. Curtis[a,b,†], Ian M. Cartwright[a,b,†], J. Scott Lee[a,b], Ruth X. Wang[a,b], Daniel J. Kao[a,b], Jordi M. Lanis[a,b], Krista M. Burney[a,b], Nichole Welch[a,b], Caroline H. T. Hall[a,b], Matthew S. Goldberg[a,b], Eric L. Campbell[a,b,c], and Sean P. Colgan[a,b,d,*]

[a]Mucosal Inflammation Program and [b]Department of Medicine, University of Colorado Anschutz Medical Campus, Aurora, CO 80045; [c]Centre for Experimental Medicine, Queen's University Belfast, Belfast BT7 1NN, Northern Ireland, UK; [d]Rocky Mountain Veterans Affairs Hospital, Denver, CO 80220

ABSTRACT **Extracellular adenosine signaling is established as a protective component in mucosal inflammatory responses. The sources of extracellular adenosine include enzymatic processing from nucleotides, such as ATP and AMP, that can be liberated from a variety of cell types, including infiltrating leukocytes. Here we demonstrate that activated human neutrophils are a source of diadenosine triphosphate (Ap3A), providing an additional source of nucleotides during inflammation. Profiling murine enteroids and intestinal epithelial cell lines revealed that intestinal epithelia prominently express apical and lateral ectonucleotide pyrophosphatase/phosphodiesterase-1 (ENPP1), a member of the ENPP family of enzymes that metabolize diadenosine phosphates, especially Ap3A. Extensions of these studies demonstrated that intestinal epithelia metabolize Ap3A to ADP and AMP, which are further metabolized to adenosine and made available to activate surface adenosine receptors. Using loss and gain of ENPP1 approaches, we revealed that ENPP1 coordinates epithelial barrier formation and promotes epithelial wound healing responses. These studies demonstrate the cooperative metabolism between Ap3A and ENPP1 function to provide a significant source of adenosine, subserving its role in inflammatory resolution.**

Monitoring Editor
Asma Nusrat
University of Michigan

Received: Jun 19, 2018
Revised: Aug 20, 2018
Accepted: Aug 27, 2018

INTRODUCTION

Acute intestinal inflammation involves the early accumulation of neutrophils (polymorphonuclear leukocytes, or PMN) followed by either resolution or progression to chronic inflammation. Transmigration of PMN to regions of injury or infection is one of the earliest manifestations of acute inflammation, necessary for host defense. Infiltration of PMN is associated with a number of chronic disease states, including ulcerative colitis and Crohn's disease (Chin and Parkos, 2007). PMN represent one of the few immune cells capable of traversing epithelia (Chin and Parkos, 2007). Crypt abscesses, a pathological hallmark of mucosal inflammation, are formed by the transmigration of PMN across the colonic crypt epithelium (Kumar *et al.*, 1982). Energy demanding processes, such as migration, phagocytosis, and the generation of reactive oxygen species, accompany the infiltration of PMN and are thought to shift the metabolic balance of tissue during inflammation (Kominsky *et al.*, 2010). Our recent studies revealed that transmigrating PMN provide a driving force for molding of the tissue environment requisite for the induction of hypoxia-inducible factor (HIF), which "transcriptionally imprints" multiple targets along the nucleotide metabolism pathway and promotes the resolution of mucosal inflammation (Campbell *et al.*, 2014).

This article was published online ahead of print in MBoC in Press (http://www.molbiolcell.org/cgi/doi/10.1091/mbc.E18-06-0377) on September 6, 2018.

†These authors contributed equally to this work.

The authors declare no financial interests in any of the work submitted here.

*Address correspondence to: Sean P. Colgan (Sean.Colgan@UCDenver.edu).

Abbreviations used: AMP, adenosine 5′-monophosphate; Ap3A, diadenosine triphosphate; CD, Crohn's disease; ENPP, ectonucleotide pyrophosphatase/phosphodiesterase; IBD, inflammatory bowel disease; IEC, intestinal epithelial cells; PMN, polymorphonuclear leukocytes; TER, transepithelial resistance.

Studies directed at understanding extracellular metabolism of nucleotides in cell and tissue responses now suggest that a number of different cells can release ATP in an active manner, particularly when O_2 levels are limited (Colgan and Taylor, 2010; Colgan and Eltzschig, 2012). It is now accepted that the major pathway for extracellular hydrolysis of ATP and ADP is the ecto-nucleoside triphosphate diphosphohydrolase (NTPDase) (Colgan and Eltzschig, 2012), previously identified as ecto-ATPase or CD39 (Gendron *et al.*, 2002; Mizumoto *et al.*, 2002). These studies indicate that ATP provides a readily available extracellular source for adenine nucleotides during hypoxia/inflammation. Ecto-5′-nucleotidase (CD73) is a membrane-bound glycoprotein that functions to hydrolyze extracellular nucleotides into bioactive nucleoside intermediates (Linden, 2001). Surface-localized CD73 converts AMP to adenosine (Ado), which in turn can activate transmembrane Ado receptors or can be internalized through dipyridamole-sensitive carriers (Colgan *et al.*, 2006). These pathways have been shown to result in such diverse endpoints as regulation of epithelial and endothelial barrier (Lennon *et al.*, 1998), stimulation of epithelial electrogenic chloride secretion (responsible for mucosal hydration) (Madara *et al.*, 1993), and promotion of lymphocyte–epithelial adhesion (Airas *et al.*, 1995). Rather little is known about the regulation of epithelial CD73 and whether this molecule contributes to mucosal barrier. Given that Ado receptor activation on epithelia (via conversion of 5′-AMP from CD73) elevates intracellular cAMP, and that elevated cAMP in epithelia promotes barrier function (Moore *et al.*, 1998; Stevens *et al.*, 2000), the possibility exists that epithelial CD73 serves a central role in permeability.

An underappreciated source of tissue nucleotides are the dinucleoside polyphosphates (DNP), a more recently identified class of nucleotides that contain two nucleosides interconnected by a variable number of phosphates (Jankowski *et al.*, 2009; Fraga and Fontes, 2011). Select members of the DNPs have been detected in human plasma, neuronal cells, endothelial cells, and platelets (Jankowski *et al.*, 2009). The DNPs have been shown to play a role in vasoregulation, neurotransmission, and cell signaling (Jankowski *et al.*, 2009). In the cardiovascular system, DNP have been shown to interfere with the function of platelets, endothelium, and smooth muscle cells (Jankowski *et al.*, 2009). The extracellular nucleoside pyrophosphatase/phosphodiesterases (ENPPs) are a group of surface-expressed enzymes with broad function and wide tissue distribution (Mackenzie *et al.*, 2012). The ENPP sequence is highly conserved between species. In humans, the ENPP family consists of five proteins of which ENPP1 and ENPP3 show similar structure/function (Mackenzie *et al.*, 2012). ENPP1 is a membrane spanning homodimer that, when cleaved, can function as a secreted circulating protein. ENPP1 is most highly expressed in vascular smooth muscle cells (VSMCs), osteoblasts, and chondrocytes (Mackenzie *et al.*, 2012). ENPPs have wide substrate specificity, and the hydrolysis of pyrophosphate bonds (i.e., ATP) and phosphodiester bonds (i.e., oligonucleotides) to produce nucleoside 5′-monophosphates (i.e., the precursor of Ado) makes ENPPs potentially quite important in extracellular nucleotide metabolism and extracellular signaling.

Here, we demonstrate that activated PMN are a source of Ap3A and that intestinal epithelial cells (IEC) express functional surface ENPP1. Loss and gain of functional ENPP1 demonstrates a central role for this Ap3A-ENPP1 axis for mucosal barrier function.

RESULTS

Activated PMN release Ap3A

Stimulated PMNs in the mucosal epithelium are a well-established source of extracellular nucleotides, including ATP, which can be further metabolized to adenosine by IEC (Madara *et al.*, 1993; Lennon *et al.*, 1998; Eltzschig *et al.*, 2006). In a high-pressure liquid chromatography (HPLC)-based screen of PMN secreted nucleotides, we identified an unknown peak that increased with PMN activation (100 nM N-formylmethionyl-leucyl-phenylalanine [fMLP]). Our past experience with multiple HPLC analyses of cell-derived nucleotides (Madara *et al.*, 1993; Lennon *et al.*, 1998; Eltzschig *et al.*, 2006; Lee *et al.*, 2018) indicated that this molecule was not a standard nucleotide (e.g., ATP, AMP, uridine-5′-triphosphate [UTP]). Purification and liquid chromatography mass spectrometry analysis of this compound identified this molecule as the dinucleotide polyphosphate Ap3A (Supplemental Figure S1), a class of nucleotides that contain two nucleosides interconnected by a variable number of phosphates (Jankowski *et al.*, 2009). As shown in Figure 1A, Ap3A release from activated PMN increased over time ($p < 0.01$ by analysis of variance [ANOVA]), reaching as much as 65 ng/ml/10^6 PMN.

Ap3A is known to be hydrolyzed to ADP and AMP by the ENPP family of enzymes. A PCR-based screen of ENPP family members on cultured IEC (including murine enteroids, T84, and Caco2 cells) revealed expression of both ENPP1 (Figure 1B) and ENPP4 (Supplemental Figure S2). Confocal immunolocalization of ENPP1 on T84 cells revealed that ENPP1 was expressed primarily on the apical and lateral membrane surfaces, with no expression on the basal membrane of polarized IEC (Figure 1, C and D, and Supplemental Figure S2). ENPP1 metabolizes Ap3A to ADP and AMP (Mackenzie *et al.*, 2012), which can be further metabolized to adenosine via CD39 and CD73, respectively (Figure 1D). Since both CD73 (Strohmeier *et al.*, 1997) and CD39 (Weissmuller *et al.*, 2008) have been reportedly expressed on IEC, we determined whether epithelial cells could metabolize Ap3A to adenosine using a sensitive functional endpoint of adenosine signaling, namely the induction of electrogenic chloride secretion (Madara *et al.*, 1993). As shown in Figure 1E, incubation of electrically confluent T84 monolayers plated on membrane permeable membrane supports with Ap3A (50 μM) rapidly induced a prominent rise in chloride efflux (measured as a short-circuit current, Isc), thereby indicating that epithelial cells rapidly metabolize Ap3A to a functional chloride secretagogue.

Ap3A responses are mediated by metabolism to adenosine

To further study IEC Ap3A responses, we sought to define a molecular marker of IEC adenosine activation as a means to examine Ap3A transcriptional regulation. Previous studies have shown that NR4A2 is an adenosine-responsive gene (Zhang *et al.*, 2010) in other cell types. Using NR4A2 transcript as a marker for adenosine signaling, we found that treatment of T84 cells with Ap3A (range 0–300 μM for 2 h) resulted in a prominent induction of NR4A2 (Figure 2A, $p < 0.001$ by ANOVA). Likewise, a time course of Ap3A (30 μM) exposure revealed a rapid induction of NR4A2 within 2 h of stimulation (Figure 2B, $p < 0.01$ by ANOVA).

To determine the relative contribution of adenosine receptors to Ap3A responses in epithelia, T84 cells were subjected to the non-metabolized adenosine receptor agonist (5′-[*N*-ethylcarboxiamido] adenosine [NECA], 10 μM for 24 h), a maneuver that desensitizes adenosine receptors, leading to their internalization and blocking of adenosine receptor-mediated responses (Strohmeier *et al.*, 1997). Under these conditions, neither adenosine nor Ap3A induced appreciable NR4A2 (Figure 2C), providing strong evidence that Ap3A activation of IEC requires metabolism to adenosine.

ENPP1 expression in IECs influences transcriptional adenosine responses

To further assess the role of ENPP1 in T84 IEC function, we targeted knockdown of ENPP1 using lentiviral short hairpin RNA (shRNA). As

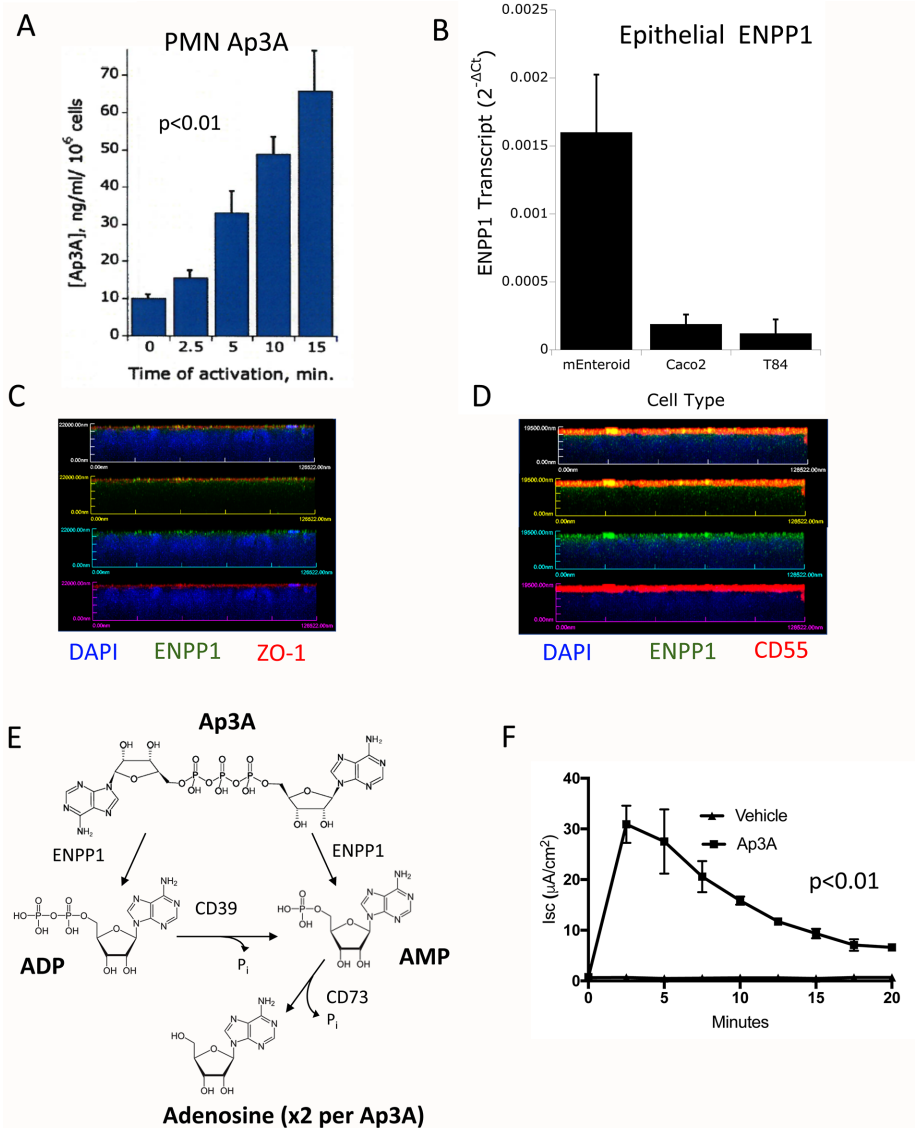

FIGURE 1: Neutrophil-derived Ap3A and expression of epithelial ENPP1. (A) Activated neutrophils (PMN) release Ap3A in a time-dependent manner ($p < 0.01$ by ANOVA). Supernatants from activated PMN were monitored for Ap3A release by HPLC analysis. (B) Epithelial cells express ENPP1. Murine enteroids, Caco2, and T84 cells were profiled for ENPP1 expression by real-time PCR. Data are expressed as ENPP1 transcript relative to β-actin. (C, D) Confocal immunolocalization of ENPP1 on T84 cells. Shown here is *x–z* plane imaging of ENPP1 (green), ZO-1 (red), CD55 (red, apical marker) (Lawrence *et al.*, 2003), and DAPI nuclear stain. (E) Depiction of Ap3A metabolism to adenosine by the concerted actions of ENPP1, CD39, and CD73. (F) Ap3A activity on epithelial electrogenic chloride secretion. Ap3A or vehicle was added to the apical and basolateral surface of confluence T84 cells and monitored for changes short circuit current (Isc) over time. Results are pooled from eight monolayers in each condition (three separate passages of cells) and expressed as the mean ± SEM ($p < 0.001$ by ANOVA).

shown in Figure 3A, this lentiviral clone decreased measurable ENPP1 mRNA by ~95% (Figure 3A, $p < 0.001$) and protein (Figure 3B) compared with shNTC (nontargeting control). Confocal immunolocalization of ENPP1 revealed significant decreases in ENPP1 compared with shNTC (Figure 3C). Treatment with Ap3A attenuated the NR4A2 response by ~50–75% in the shENPP1 cells compared with the shNTC. Likewise, knockdown of ENPP1 attenuated, but did not abolish, electrogenic chloride secretion on response to Ap3A (Figure 3E). Taken together, these results indicate that ENPP1 accounts for some, but not all, Ap3A metabolism by IECs.

To complement our loss-of-function studies, we forced overexpression of ENPP1 in T84 cells using a lentiviral vector expressing the ENPP1 open reading frame cDNA. Clones transduced with this construct (termed ENPP1-OE) expressed ~45-fold increases in ENPP1 mRNA (Figure 4A) and ~9-fold increases in ENPP1 protein by Western blot and immunolocalization (Figure 4, B and C) compared with empty vector (EV) controls. Functionally, exposure of these cells to Ap3A (30 μM) significantly enhanced both the kinetics and magnitude of chloride efflux (Figure 4D, $p < 0.001$ by ANOVA), all of which could be blocked with addition of the adenosine receptor antagonist PSB603 ($p < 0.001$ for both EV control and ENPP1-OE). Likewise, treatment of these cells with Ap3A (30 μM for 2 h) demonstrated an enhanced adenosine response in the ENPP1-OE cells with an ~3-fold higher response via NR4A2 expression compared with the EV control cells (Figure 4E). This response was specifically blocked by NECA pretreatment (Figure 4F).

To definitively demonstrate epithelial phosphohydrolysis of Ap3A to adenosine (via cooperation of ENPP1, CD39, and CD73; see Figure 5A), we adapted an established HPLC-based assay (Lee *et al.*, 2018) to monitor ENPP1-mediated metabolism of Ap3A by EV versus ENPP1-OE cells. As shown in Figure 5B, samples of Ap3A collected over time following Ap3A treatment (300 μM) revealed the appearance of ADP, AMP, and adenosine over time. A comparison of the rate of Ap3A phosphohydrolysis between ENPP1-OE and EV cells revealed increased ENPP1 activity in the ENPP1-OE cells (Figure 5C). The increased conversion of ADP and AMP to adenosine (by CD39 and CD73) was also observed in the ENPP1-OE cells compared with EV cells, likely accounting for the increased adenosine response via NR4A2 observed in the ENPP1-OE cells (Figure 4D).

Barrier formation of IECs is altered by ENPP1 expression level

We extended these studies to determine if this ENPP1-Ap3A nexus influenced epithelial functional responses. Adenosine signaling has been implicated in multiple aspects of barrier function (Lennon *et al.*, 1998; Comerford *et al.*, 2002; Lawrence *et al.*, 2002; Synnestvedt *et al.*, 2002). To examine the contribution of ENPP1, barrier formation between shNTC and shENPP1 cells was monitored over time. Monitoring transepithelial resistance (TER) over time revealed that shENPP1 cells grown on transwell inserts achieve resistance more slowly and to a lower degree compared with the shNTC cells (Figure 6A). This formation was quantified by measuring the area under the curve (AUC) and demonstrated a nearly 50% decrease compared with shNTC ($p < 0.05$, Figure 6B). Nearly identical

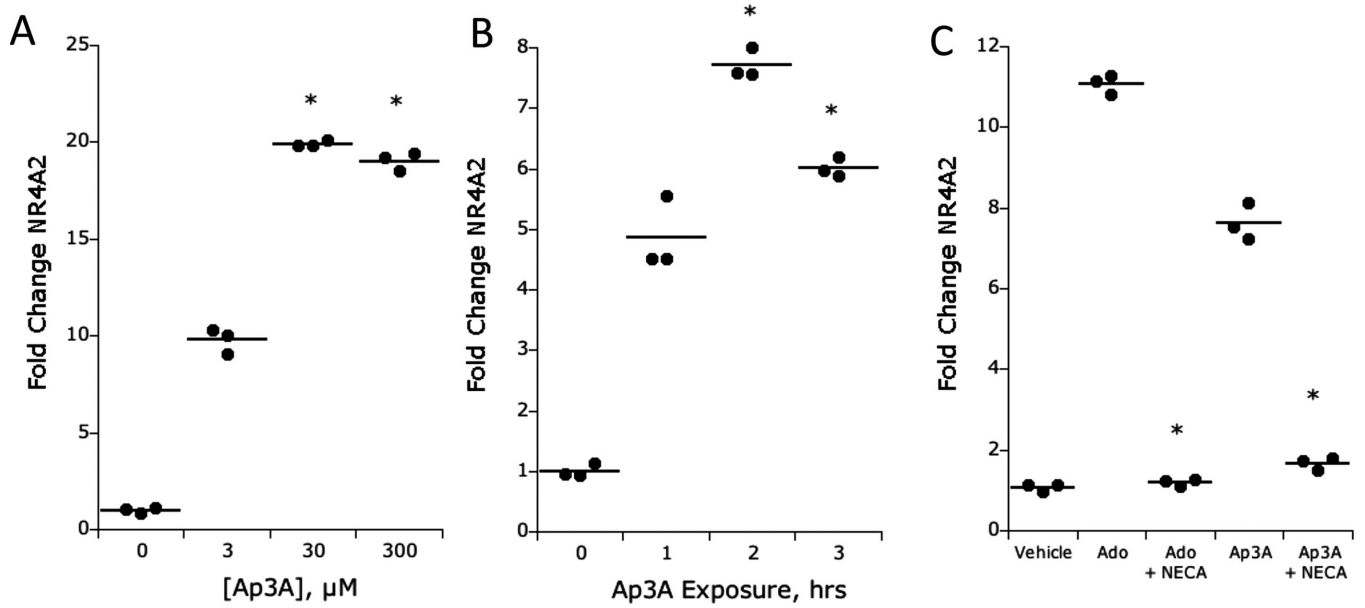

FIGURE 2: NR4A2 response to Ap3A and adenosine stimulation inT84 cells. (A) Dose response (3–300 μM) of Ap3A on NR4A2 transcriptional induction by real-time PCR. Results are expressed as the mean ± SEM of three independent experiments, where * indicates $p < 0.01$. (B) Time course of Ap3A-mediated induction of NR4A2 as determined by real-time PCR. Results are expressed as the mean ± SEM of three independent experiments, where * indicates $p < 0.01$. (C) Influence of NECA (10 μM pretreatment for 24 h) on adenosine- and Ap3A-induced NR4A2 (both at 30 μM). Results are expressed as the mean ± SEM of three independent experiments, where * indicates $p < 0.01$.

results were obtained in clustered regularly interspaced short palindromic repeats (CRISPR)-based repression of ENPP1 in T84 cells (Supplemental Figure S3). Additionally, the rate of barrier recovery in Ca^{2+} switch assays was significantly attenuated by the loss of ENPP1 cells compared with control cells ($p < 0.05$, Figure 6, C and D).

In contrast, we observed enhanced barrier formation over time in ENPP1-OE cells compared with empty vector cells (Figure 6E). When quantified, the AUC of the ENPP1-OE cells shows a significant 50% increase compared with EV cells ($p < 0.05$). These data suggest that ENPP1 expression on IECs can influence their baseline barrier integrity.

ENPP1 expression influences the migration of IEC

The migration ability of the ENPP1 knockdown and overexpression cells was measured via scratch wound assay. The shENPP1 cells demonstrated an impaired migration ability compared with the shNTC cells, as the knockdown cells only achieved an approximate 70% restitution of the wound by day 3, while the shNTC cells reached 100% restitution 2 d after wounding (Figure 7, A and B).

At baseline, there was no significant difference in wound closure between the empty vector and ENPP1-OE cells as both achieved 50% restitution 2 d after wounding. However, treatment with 30 μM Ap3A on day 0 during the assay increased the rate of restitution of both the EV and ENPP1-OE compared with untreated cells (Figure 7, C and D). The ENPP1-OE cells achieved almost 80% restitution on day 2, a significant increase compared with the EV cells treated with Ap3A. It is also notable that such increases in restitution elicited by Ap3A in ENPP1-OE and EV control cells were significantly attenuated by the addition of the adenosine A2B antagonist PSB 603 (Figure 7, E and F). These results indicate that decreased expression of ENPP1 impairs IEC migration ability while increased expression of ENPP1 in the presence of Ap3A can positively influence the migration ability.

Tight junction protein expression with ENPP1 loss and gain of function

Our observations that loss and gain of ENPP1 influence barrier function and IEC migration are further supported by expression analysis two tight junction proteins: claudin 1 (CLDN1) and claudin 2 (CLDN2). CLDN1 is known as a "tight" claudin, contributing to enhanced cell–cell junctions while CLDN2 is a "leaky" claudin, involved in paracellular channel formation. As shown in Figure 8, the expression of CLDN1 mRNA was decreased by more than 50% in shENPP1 cells compared with the shNTC cells ($p < 0.05$, Figure 8A) and significantly increased in the ENPP1-OE cells compared with the empty vector cells ($p < 0.05$, Figure 8A). Conversely, CLDN2 mRNA is significantly increased in the shENPP1 cells and significantly decreased by 40% in the ENPP1-OE cells (both $p < 0.05$, Figure 8B). These findings were confirmed by Western blot, which indicated a relative decrease in claudin-1 on cells lacking ENPP1 and a relative decrease in claudin-2 on cells overexpressing ENPP1.

Such observations were supported by immunolocalization using confocal microscopy. As shown in Figure 8, C–E, we profiled expression of the tight junction proteins ZO-1, claudin-1 and claudin-2 expression in shENPP1 knockdown and in ENPP1-OE cell lines. This analysis confirmed our mRNA and protein expression patterns, where claudin-1 trended lower and claudin-2 trended high in the shENPP1 cells. The claudin-1/-2 expression pattern was magnified in cells overexpressing ENPP1, where significant increases in claudin-1 as well as significant decreases in claudin-2 were observed compared with both empty vector controls ($p < 0.05$) and shENPP1 ($p < 0.05$) cell lines. Patterns of ZO-1 expression were not appreciably different between these cell types in *x–z* (Figure 8) or *x–y* plane (Supplemental Figure S5) imaging. These results implicate ENPP1 in the regulation of the constellation of tight junction components of established epithelial monolayers.

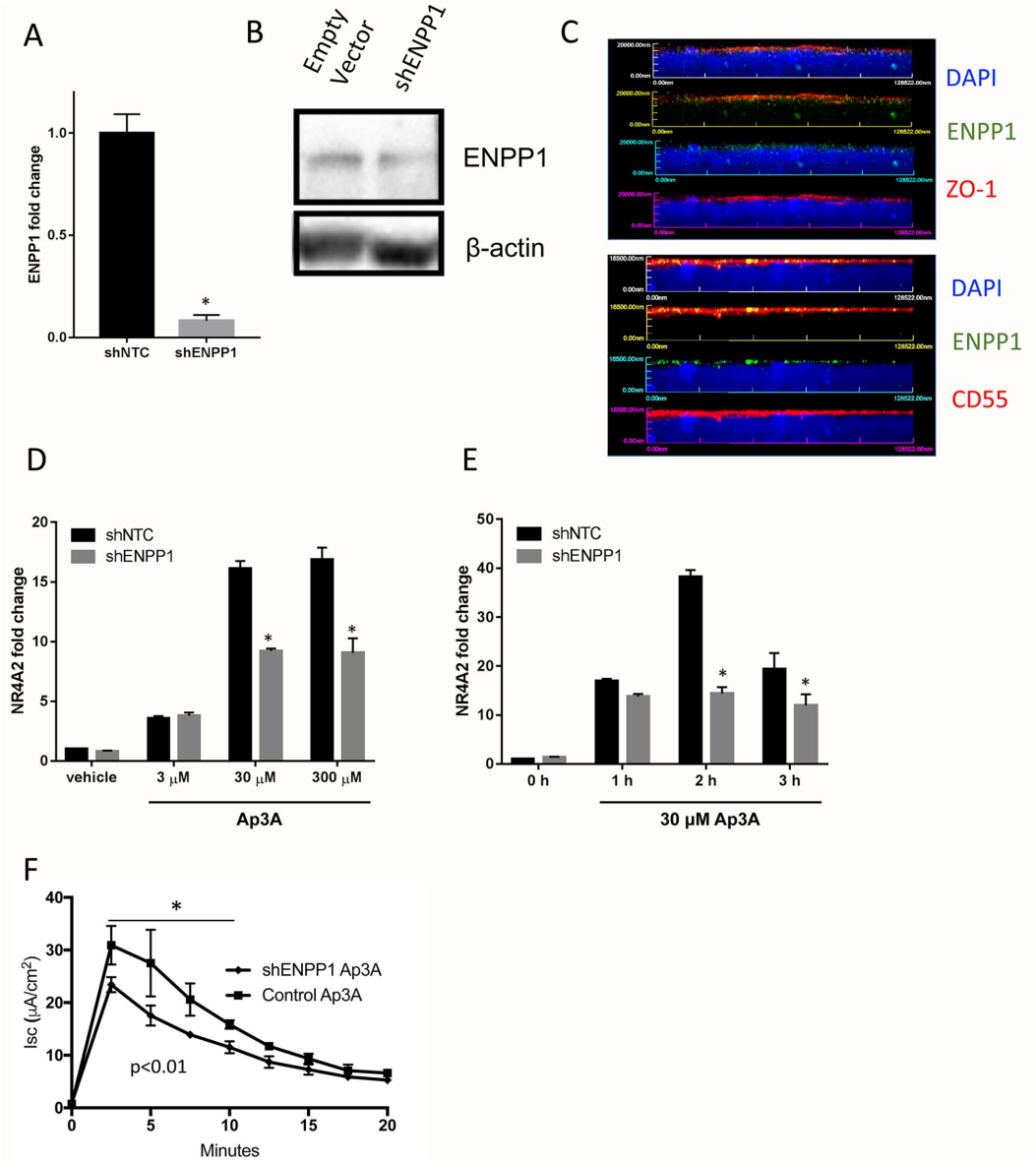

FIGURE 3: Attenuated Ap3A response in ENPP1 knockdown T84 cells. (A) Knockdown of ENPP1 was achieved using lentiviral shRNA and puromycin selection. Compared to non-targeting control (shNTC), ENPP1 transcript was decreased by ~95% (* indicates $p < 0.01$). (B) Western blot analysis of ENPP1 and β-actin from empty vector control cells and shENPP1 cells. (C) Confocal immunolocalization of ENPP1 on Empty vector (top) and shENPP1 cells. Shown here is *x–z* plane imaging of ENPP1 (green), CD55 (red, apical marker), and DAPI nuclear stain. (D) Dose response of Ap3A (3–300 μM) treatment on NR4A2 transcription. Results are expressed as the mean ± SEM of three independent experiments, where * indicates $p < 0.01$. (E) Time course of Ap3A treatment (30 μM for indicated periods of time) on NR4A2 transcription. Results are expressed as the mean ± SEM of at least three independent experiments, where * indicates $p < 0.01$. (F) Ap3A activity on epithelial electrogenic chloride secretion. Ap3A (30 μM) was added to the apical and basolateral surface of empty vector or shENPP1 cells and monitored for changes short circuit current (Isc) over time. Results are pooled from eight monolayers in each condition and expressed as the mean ± SEM ($p < 0.01$ by ANOVA).

DISCUSSION

An understanding of the metabolic responses to mucosal inflammation is an area of significant interest. Recent studies, for example, have implicated shifts in tissue metabolism as important clues that determine the overall outcomes of inflammatory responses (Taylor and Colgan, 2017). Of particular interest in the mucosa is the adaptation to "inflammatory hypoxia," wherein oxygen depletion generated by the PMN oxidative burst imprints the initiation of inflammatory resolution through the stabilization of HIF (Campbell *et al.*, 2014). In this regard, a consistent finding in inflammatory hypoxia is the generation of high levels of extracellular nucleotides that signal to the mucosa (Eltzschig *et al.*, 2012).

We demonstrate here that on activation, PMN are a prominent source of extracellular Ap3A. Consistent with prior studies suggesting that most cells contain measurable amounts of Ap3A (Ogilvie and Jakob, 1983), we show that PMN release quantifiable levels of Ap3A in an activation-dependent manner. That PMN are a source of Ap3A adds to our understanding of the importance of local

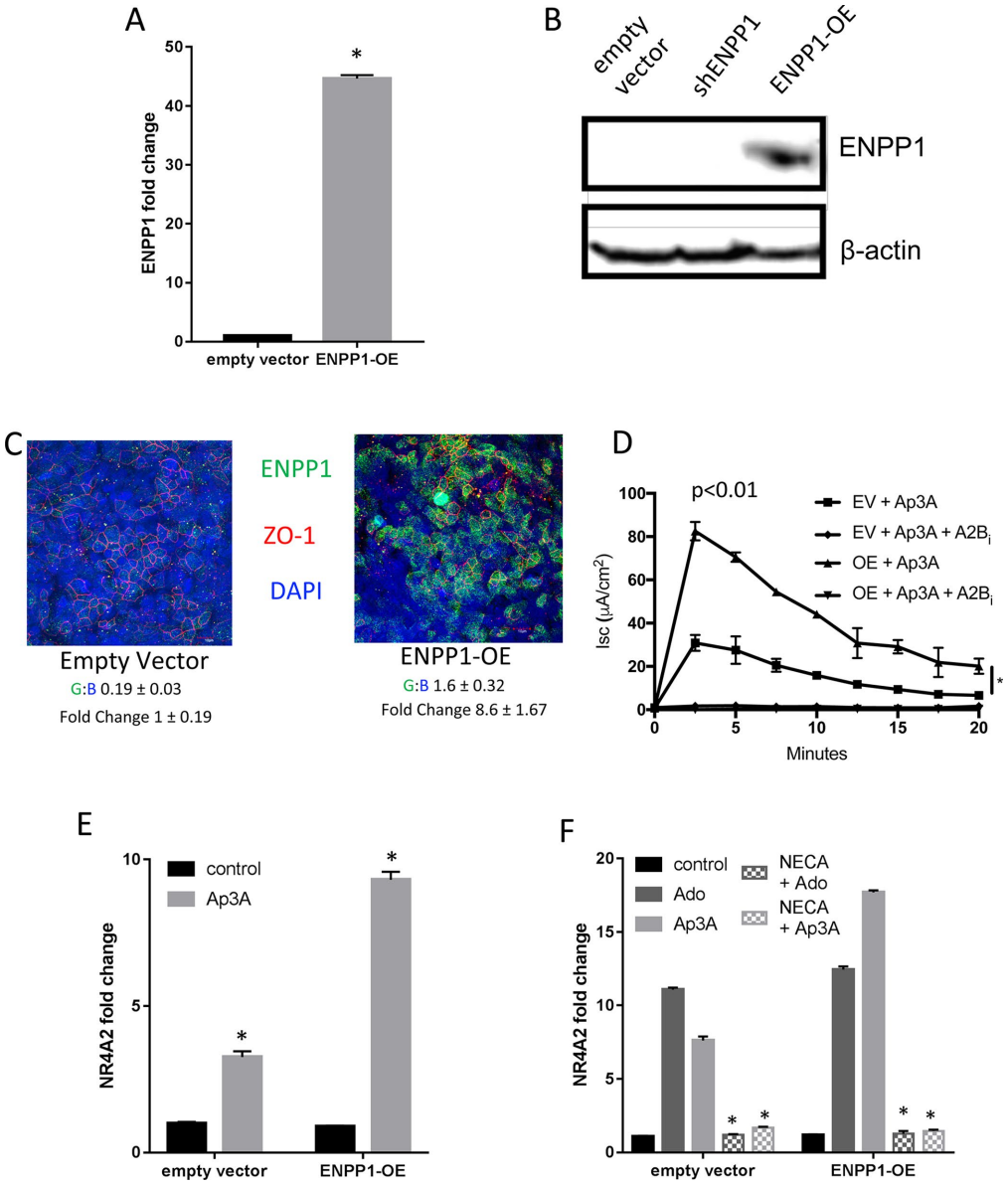

FIGURE 4: Epithelial responses to Ap3A in ENPP1 overexpressing T84 cells. (A) Real-time PCR analysis of ENPP1 in empty vector and ENPP1-OE cells, where * indicates $p < 0.01$. (B) Western blot analysis of ENPP1 in empty vector, shENPP1, and ENPP1-OE cells. β-actin loading control is also shown. (C) Confocal immunolocalization of ENPP1 in T84 cells expressing vector only or ENPP1 ORF. Below each panel is the quantification of green:blue fluorescence (G:B) and the relative change in ENPP1-OE. (D) Analysis of electrogenic chloride secretion (measured as a short circuit current, Isc) in response to Ap3A (30 μM) in Empty vector and ENPP1-OE T84 cell lines with and without addition of the adenosine A2b receptor antagonist PSB603 (A2Bi, 10 μM). Results are expressed as the mean ± SEM of three independent experiments, $p < 0.01$ by ANOVA. (E) Analysis of Ap3A response (30 μM, 2 h) as measured by NR4A2 in empty vector and ENPP1-OE cells. Results are expressed as the mean ± SEM of at least three independent experiments, where * indicates $p < 0.01$ compared with control. (F) Analysis of Ap3A response (30 μM, 2 h) as measured by NR4A2 in empty vector and ENPP1-OE cells. Results are expressed as the mean ± SEM of at least three independent experiments. Both responses were blocked by 24 h pretreatment with NECA (10 μM), where * indicates $p < 0.01$ compared with control.

nucleotide metabolism as a mechanism to promote local signaling and may potentially contribute fundamentally to inflammatory resolution. It is well documented, for instance, that PMN release other adenine nucleotides, including AMP (Madara *et al.*, 1993) and ATP (Eltzschig *et al.*, 2006), at sites of inflammation. The metabolism of these nucleotides by surface nucleotidases (e.g., CD39 and CD73) to adenosine has been shown to promote resolution through a number of mechanisms (Colgan and Eltzschig, 2012). At present, we do not know the mechanism(s) of Ap3A release from PMN. Our previous studies identified a specific role for connexin-43 (Cx43) in activation-dependent ATP release from PMN (Eltzschig *et al.*, 2006), but we do not know the specificity of Cx43 for ATP and whether nucleotides such as Ap3A could be transported. Alternatively, it is possible that Ap3A may be compartmentalized within particular granules/vesicles and released in an activation-dependent manner. It is known, for example, that Ap3A is stored within platelet dense

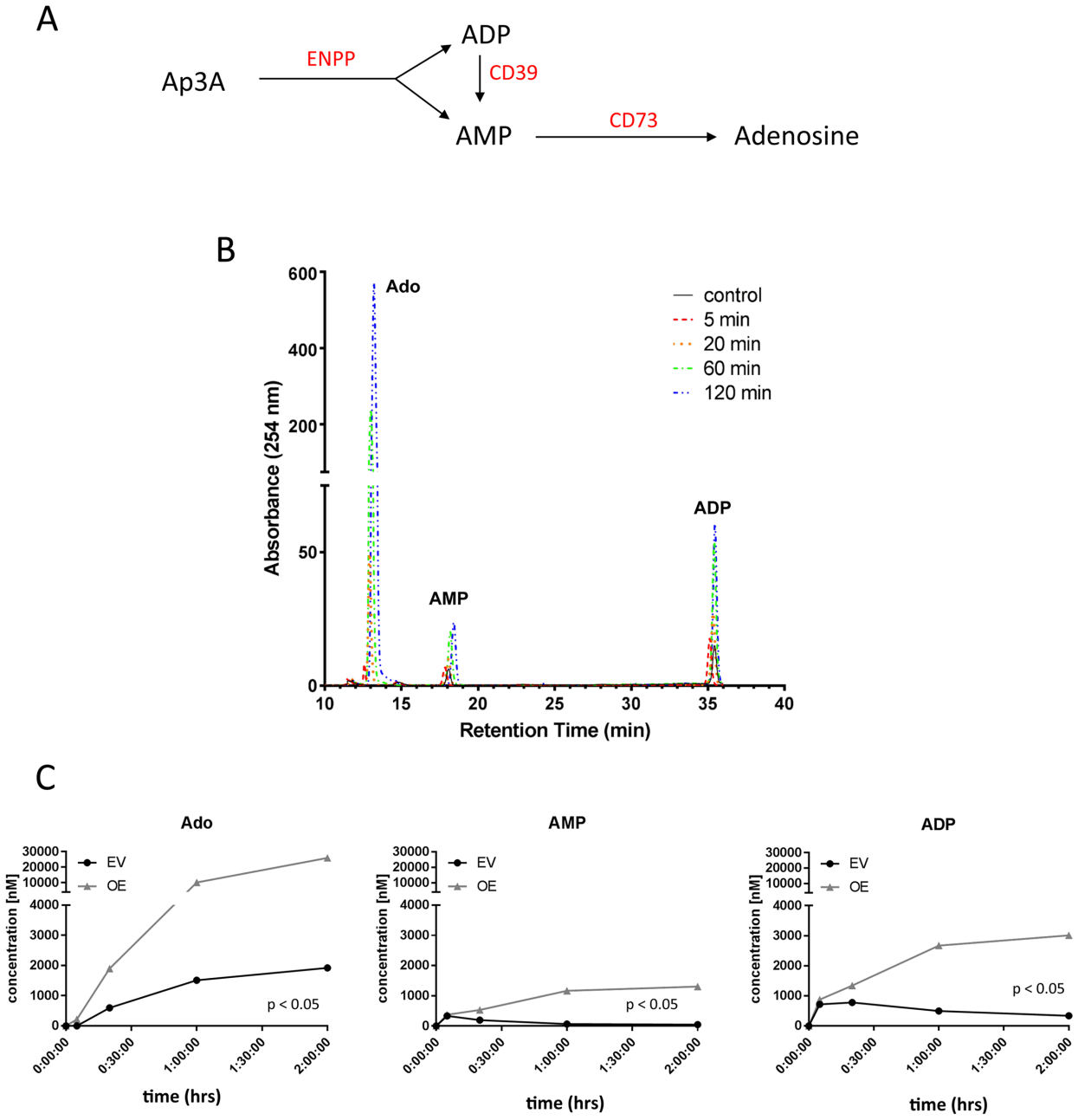

FIGURE 5: Analysis of Ap3A metabolism by epithelial cells. (A) Summary of Ap3A metabolic steps to adenosine mediated by ENPP1, CD39, and CD73. (B) HLPC tracing time course of Ap3A metabolism through ADP, AMP, and into adenosine. Individual time points are depicted in the indicated colors. (C) Analysis ADP, AMP, and adenosine in ENPP1-OE cells (gray lines) compared with empty vector cells (black lines) over a time course of Ap3A (300 μM) addition.

granules at especially high concentrations (up to 30 mM) (Luthje *et al.*, 1987) and released during platelet aggregation to promote thrombus stability. Studies are underway to understand the mechanisms of PMN Ap3A release.

These studies identify the expression of ENPP family members on intestinal epithelia and a central role for ENPP1 in metabolism of extracellular nucleotides. Guided by an initial screen of murine enteroids, we pursued the expression and function of ENPP1 in nucleotide metabolism and function in epithelia. It is notable that the expression pattern of the two ENPP family members that metabolize Ap3A (ENPP1 and ENPP4) differ between primary epithelial (i.e., enteroids) and cultured cell lines (T84 and Caco2) where enteroids express significant amounts of ENPP1 and almost no ENPP4. It was for this reason that we pursued the function of ENPP1 on IEC. ENPP1 is a membrane-spanning homodimer that is expressed in a wide range of tissues, including cartilage, heart, kidney, vascular smooth muscle, and osteoblasts and chondrocytes (Mackenzie *et al.*, 2012). The best-appreciated function of ENPP1 is in the mineralization of bone, where free phosphate derived from the action of ENPP1 on ATP or Ap3A promotes the precipitation of hydroxyapatite crystals (Mackenzie *et al.*, 2012). This function for ENPP1 has been well appreciated in Enpp1–/– mice, where extensive aortic calcification results from abnormal phosphate metabolism (Zhu *et al.*, 2011). It is noteworthy that the intestine is a major

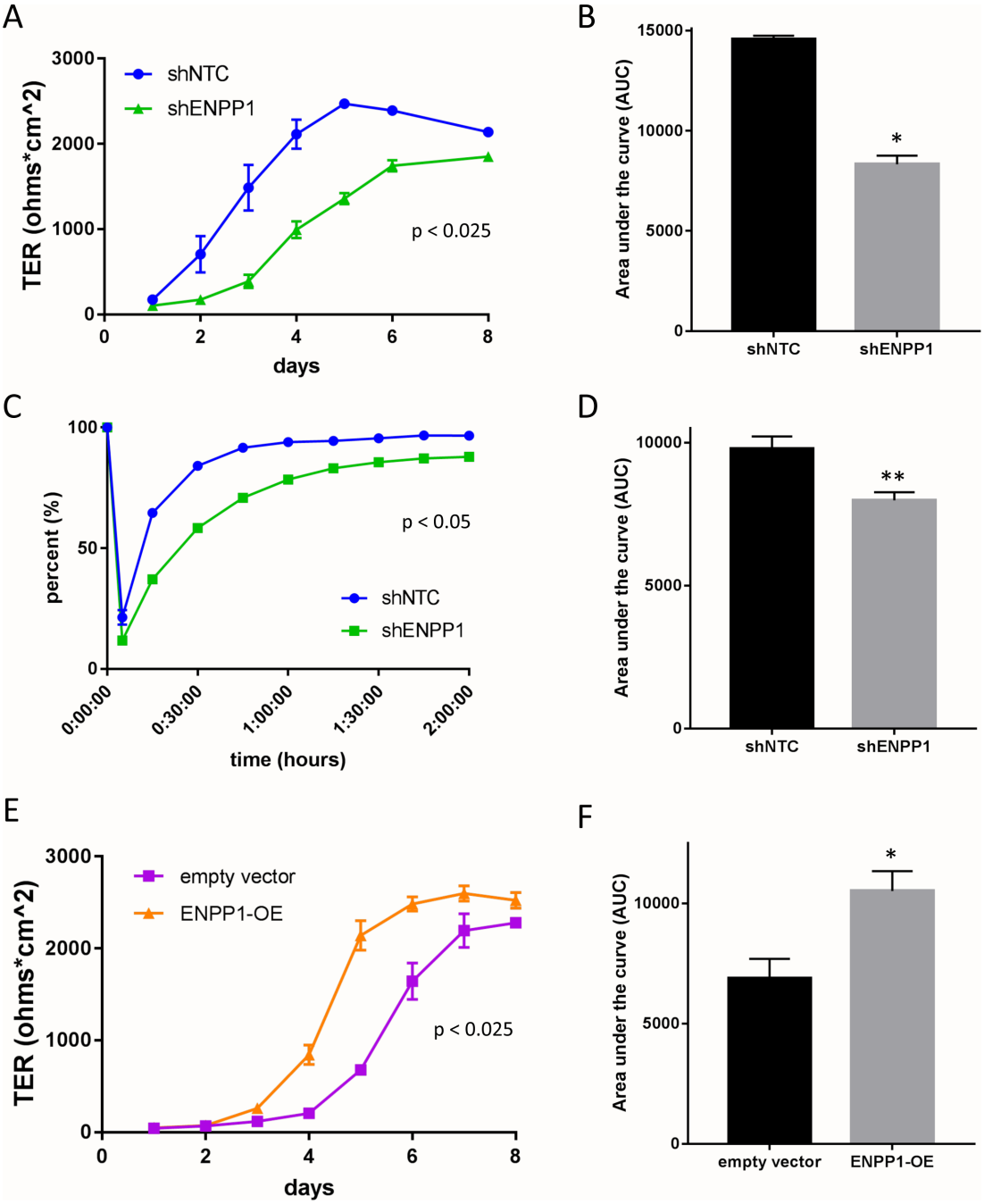

FIGURE 6: Influence of ENPP1 expression on epithelial barrier function. (A) Analysis of barrier formation over time in shNTC (blue lines) and shENPP1 KD (green lines) cells by measurement of TER ($p < 0.025$ by ANOVA). (B) Area under curve (AUC) analysis comparing shENPP1 KD cells compared with shNTC cells. Results are expressed as the mean ± SEM of at thre independent experiments, where * indicates $p < 0.01$. (C) Analysis of barrier re-formation following calcium switch assay in shNTC (blue lines) and shENPP1 KD (green lines) cells ($p < 0.05$ by ANOVA). (D) AUC analysis comparing shENPP1 KD cells compared with shNTC cells. Results are expressed as the mean ± SEM of at least three independent experiments, where ** indicates $p < 0.05$. (E) Analysis of barrier formation over time in empty vector (violet lines) and ENPP1-OE (orange lines) cells by measurement of TER ($p < 0.025$ by ANOVA). (F) AUC analysis comparing empty vector and ENPP1-OE cells. Results are expressed as the mean ± SEM of eight monolayers per condition (three separate passages of cells), where * indicates $p < 0.01$.

site of phosphate homeostasis. Uekawa *et al*. (2018) recently demonstrated that intestinal epithelial ENPP1 expression is critical for ATP metabolism and transcellular calcium transport at the luminal surface of the intestine. Consistent with our findings, they reveal that ENPP1 is expressed on the apical membrane of intestinal epithelia. With regard to nucleotide metabolism and signaling, this localization of ENPP1 at the luminal surface is important for a number of reasons. First, the major pathway for extracellular adenosine

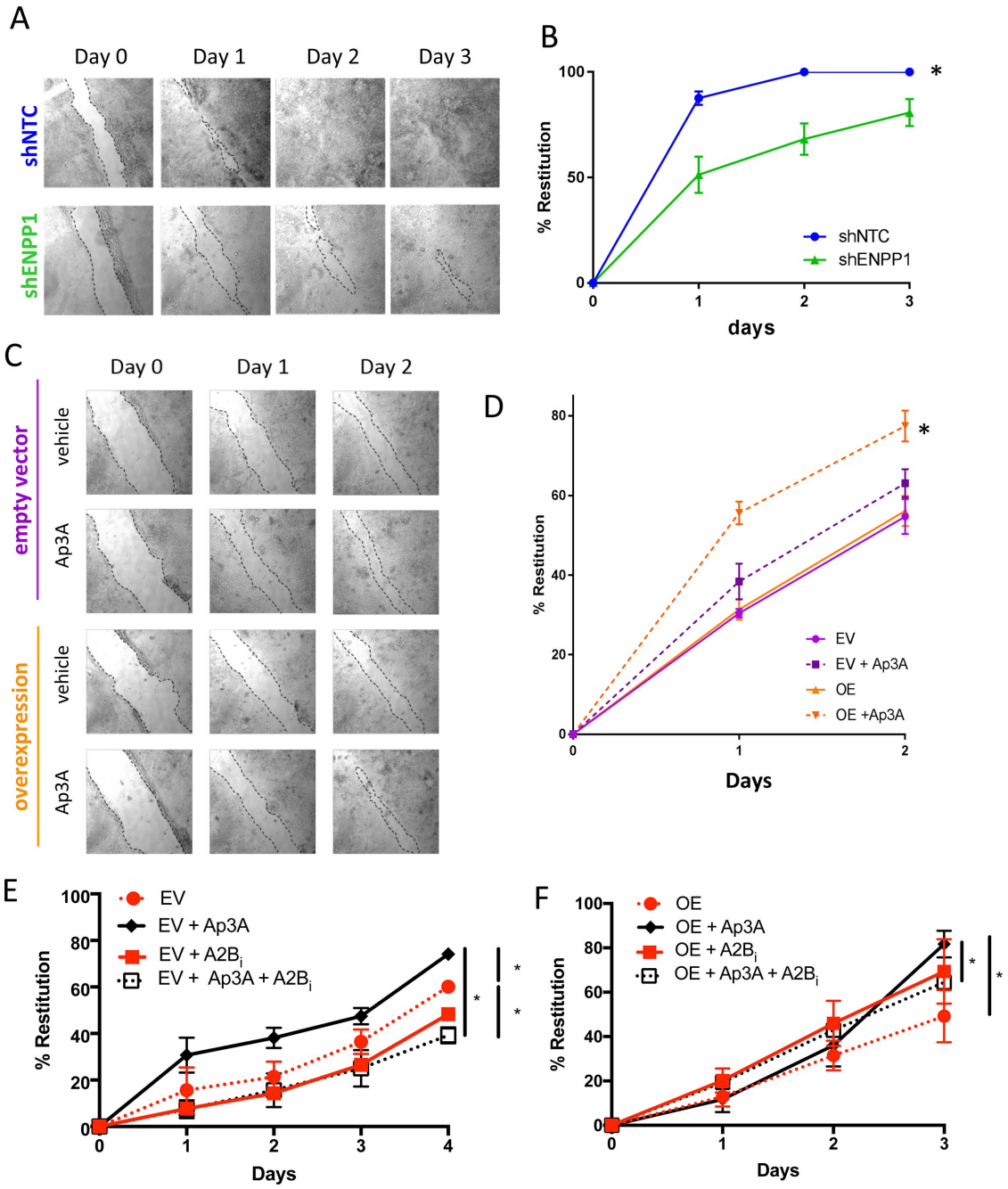

FIGURE 7: Influence of ENPP1 expression on epithelial wound healing responses. (A) Images from scratch wound assay performed with shNTC and shENPP1 cells over 3 d. (B) Analysis of measured restitution of wounded area in shENPP1 (green) cells compared with shNTC (blue) cells. Results are expressed as the mean ± SEM of seven to nine monolayers per conditions, where * indicates $p < 0.01$ by ANOVA. (C) Images from scratch wound assay performed with ENPP1-OE and empty vector cells with and without Ap3A (30 μM) addition. (D) Analysis of measured restitution of wounded area in ENPP1-OE (orange) cells compared with empty vector (violet) cells in the presence (dashed lines) and absence (solid lines) of Ap3A. Results are expressed as the mean ± SEM of six to nine monolayers per conditions (three separate passages of cells), where * indicates $p < 0.01$ by ANOVA compared with empty vector with addition of Ap3A. (E, F) Analysis of measured restitution of wounded area in Empty vector control cells (E) and ENPP1-OE cells (F) in the presence (black lines) and absence (red lines) of Ap3A with and without addition of the adenosine A2B receptor antagonist PSB603. Results are expressed as the mean ± SEM of six to nine monolayers per conditions, where * indicates $p < 0.01$ by ANOVA compared with empty vector with addition of Ap3A.

generation occurs through metabolism of AMP by CD73, a glycophosphatidylinositol-linked membrane protein that is restricted to apical expression (Strohmeier *et al.*, 1997). Past studies in mice have demonstrated that the colon expresses as much or more CD73 as any tissue in the body (Thompson *et al.*, 2004). Such membrane localization would place ENPP1 and CD73 in ideal proximity for cooperative metabolism. Second, the adenosine A2B receptor is similarly localized to the apical surface, where it is made available to activate

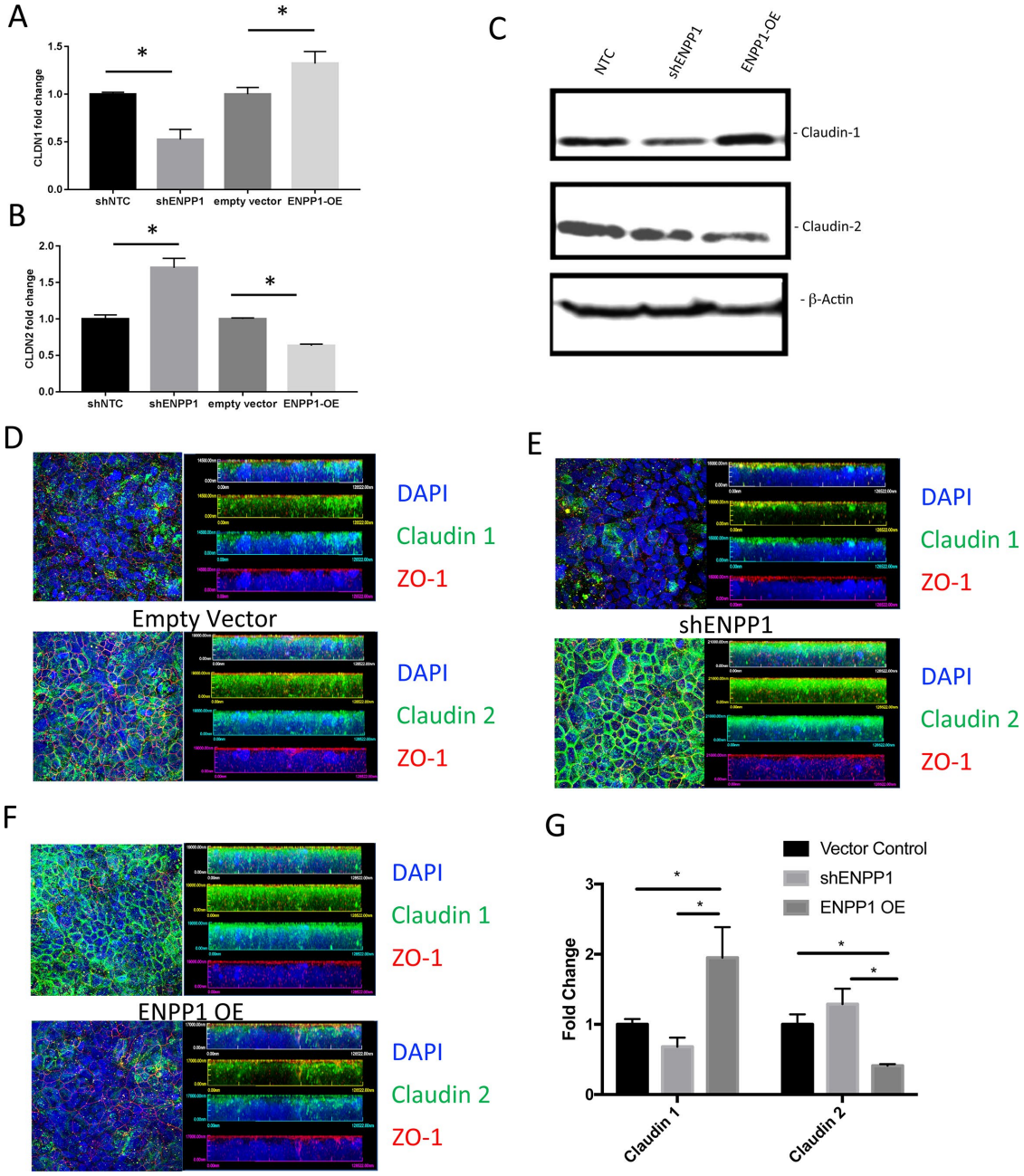

FIGURE 8: Influence of ENPP1 loss and gain of function on CLDN1 and CLDN2 expression in T84 cells. (A) Analysis of CLDN1 expression in shENPP1 cells compared with shNTC cells and in ENPP1-OE cells compared with empty vector cells (where * indicates $p < 0.025$ compared with vector control cells). (B) Analysis of CLDN2 expression in shENPP1 cells compared with shNTC cells and in ENPP1-OE cells compared with empty vector cells (where * indicates $p < 0.025$ compared with vector control cells). (C) Western blot analysis of claudin-1 and claudin-2 from lysates derived from vector controls (NTC), shENPP1 and ENPP1-OE cell lines. β-actin loading control is also shown. (D, E, F) Confocal immunolocalization of claudin-1 or claudin-2, as indicated (green) in cells expressing Empty vector only, shENPP1 or ENPP1-OE. Shown here is *x–y* plane through the tight junction and *x–z* plane imaging of claudin-1/-2 (green), ZO-1, and DAPI nuclear stain. (G) Quantification of claudin-1 and claudin-2 fluorescence signal relative to DAPI in indicated cell lines (* indicates $p < 0.05$).

signaling in epithelia (Strohmeier *et al.*, 1995). Third, during active mucosal inflammation (e.g., crypt abscess formation), the migration of PMN and platelets (Weissmuller *et al.*, 2008) across the epithelium and into the lumen of the intestine provides a particularly rich source of nucleotide precursors for metabolism along the plane of the apical epithelial surface. This new understanding that PMN are a source of secreted Ap3A implicates this domain among the most active areas of nucleotide metabolism in the body.

Signaling within the mucosa provided by PMN-derived adenosine is primarily through increases in intracellular cAMP (Colgan, 2015). Cyclic AMP signaling in proresolution pharmacology is an area of significant interest (Sousa *et al.*, 2013), and studies in the

mucosa have demonstrated that elevations in tissue cAMP promote tissue barrier through mechanisms involving increased expression of some tight junction proteins, including occludin and ZO-1 (Dye *et al.*, 2001) as well as an increase in the number of tight-junction strands (Adamson *et al.*, 1998). Increased cAMP also increases actin polymerization and phosphorylation of intermediate filaments, strongly implicating the cytoskeleton in cAMP-mediated changes in permeability (Ivanov *et al.*, 2010). Because of the actin-binding and cross-linking functions of vasodilator-stimulated phosphoprotein (VASP), it has been demonstrated that protein kinase A (PKA)-mediated VASP phosphorylation may be crucial in this pathway. In fact, VASP localizes with ZO-1 at the tight junction and appears as phospho-VASP at the junction following adenosine-mediated PKA activation in epithelia and endothelia (Comerford *et al.*, 2002; Lawrence *et al.*, 2002). Given the transient increase in epithelial permeability associated with PMN transmigration, these studies indicate that PMN-derived Ap3A provides an upstream metabolite that promotes epithelial resealing as a central component for mucosal inflammatory resolution.

Loss and gain of ENPP1 function approaches in intestinal epithelia revealed a central role for ENPP1 signaling in epithelium barrier function and wound healing, where ENPP1 expression strongly correlated with enhanced barrier function. It is notable that even at baseline (i.e., without exogenous Ap3A), knockdown of ENPP1 diminished the ability of epithelia to form barrier. Such results suggest that epithelia themselves release Ap3A or, more likely, ATP during barrier formation that is subsequently metabolized to AMP and adenosine. One noteworthy caveat to our work here is the recognition that lentiviral knockdown of ENPP1 does not result correlative loss of ENPP surface activity. Our results, in fact, indicate that T84 cells may actually express more ENPP4 than ENPP1. For this reason, it is likely that the significant residual signaling by Ap3A (e.g., NR4A2 induction, Cl- secretion) in shENPP1 could reflect the compensation by ENPP4.

Our studies also indicate that ENPP1 expression correlates with a pattern of claudin expression in support of enhanced barrier, namely increased claudin-1 and decreased claudin-2 (Capaldo and Nusrat, 2015). As a "tight claudin," CLDN1 plays an integral role in determining barrier function in IECs (Inai *et al.*, 1999) and is a marker of differentiation in the squamous epithelium of the esophagus. CLDN2 has been described as a "leaky claudin" that loosens tight junctions. At baseline in the mucosa, claudin-2 is restricted to proliferative colonic crypt base epithelia. During mucosal inflammation, claudin-2 expression is strongly induced, and the expression pattern extends well beyond the proliferative zone and along the crypt–villus axis (Capaldo and Nusrat, 2015). Changes in tight junction profiles of claudins (i.e., claudin remodeling) can be influenced by many factors, including transcriptional regulation, posttranslational modifications, and stabilization within the plasma membrane (Garcia-Hernandez *et al.*, 2017). Claudin-2 is also strongly induced by some proinflammatory cytokines. Essentially nothing is known about how AP3A/adenosine signaling might influence the expression of claudin-1/-2. One study suggests that protein kinase A (PKA) activation results in increased cytoplasmic claudin-1 expression and that cells transfected with claudin-1 mutants lacking PKA docking sites demonstrated decreased motility (French *et al.*, 2009), which would be consistent with our scratch wound assays. More work is necessary to define the precise contribution of this Ap3A/ENPP complex to the regulation of claudin expression in IEC.

Despite its importance, little is known about the transcriptional regulation of CLDN1. A number of studies have implicated other surface enzymes (e.g., CD39 and CD73) in the control of tissue barrier function, particularly during hypoxia (Colgan *et al.*, 2016). Successful transmigration of leukocytes, especially PMN, across epithelial and endothelial monolayers is accomplished by temporary self-deformation with localized widening of the interjunctional spaces (Chin and Parkos, 2007), a process with the potential to disturb endothelial and epithelial barrier function. Thus, given its anatomic location and expression pattern, ENPP1 may function to orchestrate barrier responses during inflammation.

In summary, our results highlight for the first time the active release of Ap3A from PMN and provide a new pathway for the production of extracellular nucleotides during active inflammatory responses. Such Ap3A is rapidly hydrolyzed to adenosine via close association with CD73 expressing cell types, such as intestinal epithelia. This PMN-epithelial cross-talk mechanism may play an important role in the metabolic control of innate inflammatory pathways.

MATERIALS AND METHODS

PMN isolation and stimulation

Human neutrophils were isolated from whole venous blood of healthy volunteers as described in detail previously (Campbell *et al.*, 2007). Briefly, whole venous blood was collected in syringes containing anticoagulant (K_2EDTA at 1.8 mg/ml blood). Blood was gently layered over double-density Histopaque gradients (1119/1077) and centrifuged at 700 × *g* in a swinging bucket rotor centrifuge for 30 min without brake. The resulting buffy coat was collected, and residual red blood cells were lysed. PMN were washed with ice-cold Hanks buffered saline solution (HBSS) (without $CaCl_2$ or $MgCl_2$), counted, and used within 2 h of isolation.

Samples of PMN (1×10^7/ml) were stimulated with fMLP (100 nM in HBSS) for variable periods of time. Samples were centrifuged, filtered, and analyzed by HPLC (Lee *et al.*, 2018). For further purification, HPLC eluted samples were collected, concentrated by vacufuge, and submitted to the University of Colorado Biological Mass Spectrometry Core Facility for analysis.

Cell culture

Human T84 intestinal epithelial cells were cultured in 95% air with 5% CO_2 at 37°C in DMEM and DMEM:F12, respectively, supplemented with 10% calf serum (Thermo Fisher Scientific, Waltham, MA) and penicillin/streptomycin (100 U/ml,100 µg/ml; Invitrogen, Carlsbad, CA). Murine enteroids were isolated from wild-type C57Bl/6 mice and cultured as previously described (Miyoshi and Stappenbeck, 2013). Briefly, minced colonic tissue was enzymatically digested and dissociated in GentleMACS tubes (Milteny Biotec, San Diego, CA), filtered through a 70-µm cell strainer, and resuspended in Matrigel (Corning, Corning, NY). Cells were cultured in L-WRN conditioned media.

Lentiviral particles encoding shRNA against ENPP1 (MISSION TRC shRNA; Sigma-Aldrich, St. Louis, MO) or an ENPP1 ORF (Origene, Rockville, MD) were transduced into T84 cells using established protocols to derive shENPP1 (and shNon-Targeting Control or shNTC) and ENPP1-overexpression (ENPP1-OE; and empty vector or EV) cell lines.

As a complementary approach, ENPP1 repression was also achieved using CRISPR. Specifically, single-guide RNA (sgRNA) sequence targeting the gene was generated by the Functional Genomic Core at the University of Colorado, Denver. The sgRNA sequence used to target ENPP1 was 5′-CACCGAGGTCATCAAAGCCTTGCAG. The sgRNA oligos were ligated into the lentiCRISPR v2 vector (Sanjana *et al.*, 2014), which coexpresses cas9 and sgRNA in the same vector. The CRISPR lentivirus vector was then packaged according to a

standard protocol. To produce lentiviral vectors, lentiviral plasmids with the target sgRNA were transduced into HEK293T cells together with second-generation packaging plasmids (psPAX2 and pMD2.G) following previously published procedures (Zhang *et al.*, 2017). The collected virus was placed on 60–70% confluent T84 cells along with 10 μg/ml polybrene and incubated for 24 h. After 24 h, the medium was replaced with fresh M4 and incubated for another 24 h. M4 containing 6 μg/ml puromycin was added to the cells. After 7 d of selection, cells were collected and assayed for ENPP1 knockout via Western blot.

Transcriptional analysis

TRIzol reagent (Invitrogen) was used to isolate RNA from Caco-2 or T84 cells. cDNA was reverse transcribed using the iScript cDNA Synthesis Kit (Bio-Rad, Hercules, CA). PCR analysis was performed using SYBR Green (Applied Biosystems, Carlsbad, CA) and the following primer sequences: ENPP1, forward, 5′-TTACCAGGAGACGTGCATAGA-3′, reverse, 5′-GGTCAACCTTTTCTCACCACAC-3′, NR4A2, forward, 5′-GTTCAGGCGCAGTATGGGTC-3′, reverse, 5′-CTCCCGAAGAGTG GTAACTGT-3′, and β-actin, forward, 5′-GCACTCTTCCAGCCTTCCT TCC-3′, reverse, 5′-CAGGTCTTTGCGGATGTCCACG-3′. Each experiment was performed in triplicate.

HPLC analysis

T84 EV and ENPP1-OE were plated on 5-cm^2 inserts (Corning) and grown to resistance (>1000 ohms·cm^2). The inserts were then washed, equilibrated in HBSS+, and treated apically and basolaterally with 300 μM Ap3A (Sigma-Aldrich). Aliquots of equivalent volumes were sampled both apically and basolaterally at 5, 20, 60, and 120 min. The samples were flash frozen in liquid nitrogen and stored at –80°C until analyzed by HPLC.

Purines were quantified as described elsewhere (Lee *et al.*, 2018). Briefly, analyses were performed on an Agilent Technologies 1260 Infinity HPLC using a C18 column (100 Å, 150 × 4.6 mm with mobile phase A: 50 mM KH_2PO_4, 5 mM tetrabutylammonium bisulfate, pH 6.25; mobile phase B: acetonitrile; column temperature: 30°C; flow rate: 1 ml/min; 75 μl injection). Samples were filtered through VIVASPIN 500 membranes (Sartorius Stedim Biotech, 5000 MWCO, PES) prior to HPLC analysis. Chromatographic separation of the metabolites was performed using a combination of isocratic and gradient methods including column washing and equilibration periods at the end (0 min: 100% A; 7 min: 100% A; 10 min: 97% A; 18 min: 97% A; 45 min: 86% A; 60 min: 50% A; 80 min: 50% A; 90 min: 100% A; 135 min: 100% A). The metabolites were detected by absorption at 254 nm, with their absorbance spectra and retention times verified by coinjection with authentic standards.

Western blot

Proteins were solubilized in Laemmli sample buffer. Samples were not heated to avoid protein aggregation and up to 100 μg/lane were resolved on a 7.5% polyacrylamide gel and transferred to polyvinylidene fluoride membranes. The membranes were blocked 1 h at room temperature (RT) in phosphate-buffered saline (PBS) supplemented with 0.2% Tween-20 (PBS-T) and 4% bovin serum albumin. Membranes were incubated with anti-ENPP1 rabbit polyclonal antibody (L520; Cell Signaling Technology, Danvers, MA) or rabbit polyclonal anti-β-actin (Abcam, Cambridge, UK) in PBS-T for 1 h at RT, followed by 3- to 10-min washes in PBS-T. Membranes were then incubated with peroxidase conjugated goat-anti-mouse immunoglobulin G (110 ng/ml; ICN/Cappel, Cosa Mesa, CA) for 1 h at RT. After the wash was repeated, proteins were detected by enhanced chemiluminescence.

Immunofluorescence

Immunolocalization and confocal imaging were performed as previously described (Glover *et al.*, 2013). Briefly, T84 cells were plated on small (0.33-cm^2, 0.4 μM permeable polyester) inserts (Corning) and grown until electrically confluent (7–10 d). The inserts were removed and briefly washed with PBS three times. The inserts were fixed with 4% paraformaldehyde for 15 min and washed three times in PBS for 5 min. Inserts were blocked in PBS containing 10% goat serum for 1 h at RT. Inserts were incubated with anti-ZO-1 or anti-CD55 mouse antibody with anti-ENPP1, anti-Claudin1, or anti-Claudin2 rabbit antibodies for 1 h at RT. The inserts were washed three times in PBS for 5 min and incubated in PBS containing 10% goat serum and 1:1000 Alexafluor 488 and Alexafluor 555 for 1 h at RT. The inserts were briefly washed three times in PBS. The membrane was removed from the insert and mounted onto a slide with 10 μl ProLong gold antifade with 4′,6-diamidino-2-phenylindole (DAPI) (Invitrogen). Slides where image using an Olympus FV1000 confocal laser scanning microscope with 405-nm, 488-nm, and 543-nm lasers. Excitation and Emission spectra was taken into account to limit spectral bleed. Z-stacks were captured using a Z-step of 0.5 nm.

Barrier formation and calcium switch assays

T84 cells were plated on small (0.33-cm^2, 0.4 μM permeable polyester) inserts (Corning). TER was measured using the EVOM2 voltohmmeter (World Precision Instruments, Sarasota, FL) to monitor barrier formation over time. For the Ca^{2+} switch assays, T84 cells (shNTC and shENPP1) were grown to confluence on small inserts. Calcium switch was performed by equilibrating cells in HBSS+ for 20 min and then incubating the cells in Ca^{2+} free HBSS (HBSS-) with 2 mM EDTA for 5 min. The cells were then returned to HBSS+ alone. TER was measured using the EVOM2. Area under the curve (AUC) was calculated and compared between groups.

Scratch wound assay

T84 cells (shNTC/shENPP1 and empty vector/ENPP1-OE) were grown to confluence on six-well plates. The monolayers were scratched with a gel-loading pipette tip with two scratches per well. The scratched well were washed with PBS and replaced with fresh media. For empty vector/ENPP1-OE cells, 30 M Ap3A was added to the fresh media of half the well. Photographs of the scratches were taken immediately as "Day 0" and every 24 h for 2–3 additional days using a Diaphot inverted tissue culture microscope and camera system (Nikon, Tokyo, Japan). The wound restitution was calculated after measuring the wound distances using the SPOT software (SPOT Imaging, Sterling Heights, MI).

Statistical analysis

Data are expressed as mean values ± SEM. Data were analyzed with Student's *t* test between two groups or ANOVA coupled with post-hoc Bonferroni test for multiple pairwise comparisons. Probability values of $p < 0.05$ were considered to be statistically significant.

ACKNOWLEDGMENTS

This work was supported by National Institutes of Health grants DK1047893, DK50189, DK095491, and DK103712 and by Veterans Administration Merit Award BX002182.

REFERENCES

Adamson RH, Liu B, Fry GN, Rubin LL, Curry FE (1998). Microvascular permeability and number of tight junctions are modulated by cAMP. Am J Physiol 274, H1885–H1894.

Airas L, Hellman J, Salmi M, Bono P, Puurunen T, Smith DJ, Jalkaanen S (1995). CD73 is involved in lymphocyte binding to the endothelium:

characterization of lymphocyte-vascular adhesion protein 2 identifies it as CD73. J Exp Med 182, 1603–1608.
Campbell EL, Bruyninckx WJ, Kelly CJ, Glover LE, McNamee EN, Bowers BE, Bayless AJ, Scully M, Saeedi BJ, Golden-Mason L, *et al*. (2014). Transmigrating neutrophils shape the mucosal microenvironment through localized oxygen depletion to influence resolution of inflammation. Immunity 40, 66–77.
Campbell EL, Louis NA, Tomassetti SE, Canny GO, Arita M, Serhan CN, Colgan SP (2007). Resolvin E1 promotes mucosal surface clearance of neutrophils: a new paradigm for inflammatory resolution. FASEB J 21, 3162–3170.
Capaldo CT, Nusrat A (2015). Claudin switching: physiological plasticity of the Tight Junction. Semin Cell Dev Biol 42, 22–29.
Chin AC, Parkos CA (2007). Pathobiology of neutrophil transepithelial migration: implications in mediating epithelial injury. Annu Rev Pathol 2, 111–143.
Colgan SP (2015). Neutrophils and inflammatory resolution in the mucosa. Semin Immunol 27, 177–183.
Colgan SP, Campbell EL, Kominsky DJ (2016). Hypoxia and mucosal inflammation. Annu Rev Pathol 11, 77–100.
Colgan SP, Eltzschig HK (2012). Adenosine and hypoxia-inducible factor signaling in intestinal injury and recovery. Annu Rev Physiol 74, 153–175.
Colgan SP, Eltzschig HK, Eckle T, Thompson LF (2006). Physiological roles for ecto-5′-nucleotidase (CD73). Purinergic Signal 2, 351–360.
Colgan SP, Taylor CT (2010). Hypoxia: an alarm signal during intestinal inflammation. Nat Rev Gastroenterol Hepatol 7, 281–287.
Comerford KM, Lawrence DW, Synnestvedt K, Levi BP, Colgan SP (2002). Role of vasodilator-stimulated phosphoprotein in PKA-induced changes in endothelial junctional permeability. FASEB J 16, 583–585.
Dye JF, Leach L, Clark P, Firth JA (2001). Cyclic AMP and acidic fibroblast growth factor have opposing efffects on tight and adherens junctions in microvascular endothelial cells in vitro. Microvasc Res 62, 94–113.
Eltzschig HK, Eckle T, Mager A, Kuper N, Karcher C, Weissmuller T, Boengler K, Schulz R, Robson SC, Colgan SP (2006). ATP release from activated neutrophils occurs via connexin 43 and modulates adenosine-dependent endothelial cell function. Circ Res 99, 1100–1108.
Eltzschig HK, Sitkovsky MV, Robson SC (2012). Purinergic signaling during inflammation. N Engl J Med 367, 2322–2333.
Fraga H, Fontes R (2011). Enzymatic synthesis of mono and dinucleoside polyphosphates. Biochim Biophys Acta 1810, 1195–1204.
French AD, Fiori JL, Camilli TC, Leotlela PD, O'Connell MP, Frank BP, Subaran S, Indig FE, Taub DD, Weeraratna AT (2009). PKC and PKA phosphorylation affect the subcellular localization of claudin-1 in melanoma cells. Int J Med Sci 6, 93–101.
Garcia-Hernandez V, Quiros M, Nusrat A (2017). Intestinal epithelial claudins: expression and regulation in homeostasis and inflammation. Ann NY Acad Sci 1397, 66–79.
Gendron FP, Benrezzak O, Krugh BW, Kong Q, Weisman GA, Beaudoin AR (2002). Purine signaling and potential new therapeutic approach: possible outcomes of NTPDase inhibition. Curr Drug Targets 3, 229–245.
Glover LE, Bowers BE, Saeedi B, Ehrentraut SF, Campbell EL, Bayless AJ, Dobrinskikh E, Kendrick AA, Kelly CJ, Burgess A, *et al*. (2013). Control of creatine metabolism by HIF is an endogenous mechanism of barrier regulation in colitis. Proc Natl Acad Sci USA 110, 19820–19825.
Inai T, Kobayashi J, Shibata Y (1999). Claudin-1 contributes to the epithelial barrier function in MDCK cells. Eur J Cell Biol 78, 849–855.
Ivanov AI, Parkos CA, Nusrat A (2010). Cytoskeletal regulation of epithelial barrier function during inflammation. Am J Pathol 177, 512–524.
Jankowski V, van der Giet M, Mischak H, Morgan M, Zidek W, Jankowski J (2009). Dinucleoside polyphosphates: strong endogenous agonists of the purinergic system. Br J Pharmacol 157, 1142–1153.
Kominsky DJ, Campbell EL, Colgan SP (2010). Metabolic shifts in immunity and inflammation. J Immunol 184, 4062–4068.
Kumar NB, Nostrant TT, Appelman HD (1982). The histopathologic spectrum of acute self-limited colitis (acute infectious type colitis). Am J Surg Pathol 6, 523–529.
Lawrence DW, Bruyninckx WJ, Louis NA, Lublin DM, Stahl GL, Parkos CA, Colgan SP (2003). Anti-adhesive role of apical decay-accelerating factor (DAF, CD55) in human neutrophil transmigration across mucosal epithelia. J Exp Med 198, 999–1010.
Lawrence DW, Comerford KM, Colgan SP (2002). Role of VASP in reestablishment of epithelial tight junction assembly after Ca2+ switch. Am J Physiol Cell Physiol 282, C1235–C1245.
Lee JS, Wang RX, Alexeev EE, Lanis JM, Battista KD, Glover LE, Colgan SP (2018). Hypoxanthine is a checkpoint stress metabolite in colonic epithelial energy modulation and barrier function. J Biol Chem 293, 6039–6051.
Lennon PF, Taylor CT, Stahl GL, Colgan SP (1998). Neutrophil-derived 5′-adenosine monophosphate promotes endothelial barrier function via CD73-mediated conversion to adenosine and endothelial A_{2B} receptor activation. J Exp Med 188, 1433–1443.
Linden J (2001). Molecular approach to adenosine receptors: receptor-mediated mechanisms of tissue protection. Annu Rev Pharmacol Toxicol 41, 775–787.
Luthje J, Miller D, Ogilvie A (1987). Unproportionally high concentrations of diadenosine triphosphate (Ap3A) and diadenosine tetraphosphate (Ap4A) in heavy platelets. Consequences for in vitro studies with human platelets. Blut 54, 193–200.
Mackenzie NC, Huesa C, Rutsch F, MacRae VE (2012). New insights into NPP1 function: lessons from clinical and animal studies. Bone 51, 961–968.
Madara JL, Patapoff TW, Gillece-Castro B, Colgan SP, Parkos CA, Delp C, Mrsny RJ (1993). 5′-adenosine monophosphate is the neutrophil-derived paracrine factor that elicits chloride secretion from T84 intestinal epithelial cell monolayers. J Clin Invest 91, 2320–2325.
Miyoshi H, Stappenbeck TS (2013). In vitro expansion and genetic modification of gastrointestinal stem cells in spheroid culture. Nat Protoc 8, 2471–2482.
Mizumoto N, Kumamoto T, Robson SC, Sevigny J, Matsue H, Enjyoji K, Takashima A (2002). CD39 is the dominant Langerhans cell-associated ecto-NTPDase: modulatory roles in inflammation and immune responsiveness. Nat Med 8, 358–365.
Moore TM, Chetham PM, Kelly JJ, Stevens T (1998). Signal transduction and regulation of lung endothelial cell permeability. Interaction between calcium and cAMP. Am J Physiol 275, L203–L222.
Ogilvie A, Jakob P (1983). Diadenosine 5′,5"′-P1,P3-triphosphate in eukaryotic cells: identification and quantitation. Anal Biochem 134, 382–392.
Sanjana NE, Shalem O, Zhang F (2014). Improved vectors and genome-wide libraries for CRISPR screening. Nat Methods 11, 783–784.
Sousa LP, Alessandri AL, Pinho V, Teixeira MM (2013). Pharmacological strategies to resolve acute inflammation. Curr Opin Pharmacol 13, 625–631.
Stevens T, Garcia JGN, Shasby DM, Bhattacharya J, Malik AB (2000). Mechanisms regulating endothelial cell barrier function. Am J Physiol (Lung Cell Mol Physiol) 279, L419–L422.
Strohmeier GR, Lencer WI, Patapoff TW, Thompson LF, Carlson SL, Moe SJ, Carnes DK, Mrsny RJ, Madara JL (1997). Surface expression, polarization, and functional significance of CD73 in human intestinal epithelia. J Clin Invest 99, 2588–2601.
Strohmeier GR, Reppert SM, Lencer WI, Madara JL (1995). The A2b adenosine receptor mediates cAMP responses to adenosine receptor agonists in human intestinal epithelia. J Biol Chem 270, 2387–2394.
Synnestvedt K, Furuta GT, Comerford KM, Louis N, Karhausen J, Eltzschig HK, Hansen KR, Thompson LF, Colgan SP (2002). Ecto-5′-nucleotidase (CD73) regulation by hypoxia-inducible factor-1 mediates permeability changes in intestinal epithelia. J Clin Invest 110, 993–1002.
Taylor CT, Colgan SP (2017). Regulation of immunity and inflammation by hypoxia in immunological niches. Nat Rev Immunol 17, 774–785.
Thompson LF, Eltzschig HK, Ibla JC, Van De Wiele CJ, Resta R, Morote-Garcia JC, Colgan SP (2004). Crucial role for ecto-5′-nucleotidase (CD73) in vascular leakage during hypoxia. J Exp Med 200, 1395–1405.
Uekawa A, Yamanaka H, Lieben L, Kimira Y, Uehara M, Yamamoto Y, Kato S, Ito K, Carmeliet G, Masuyama R (2018). Phosphate-dependent luminal ATP metabolism regulates transcellular calcium transport in intestinal epithelial cells. FASEB J 32, 1903–1915.
Weissmuller T, Campbell EL, Rosenberger P, Scully M, Beck PL, Furuta GT, Colgan SP (2008). PMNs facilitate translocation of platelets across human and mouse epithelium and together alter fluid homeostasis via epithelial cell-expressed ecto-NTPDases. J Clin Invest 118, 3682–3692.
Zhang L, Paine C, Dip R (2010). Selective regulation of nuclear orphan receptors 4A by adenosine receptor subtypes in human mast cells. J Cell Commun Signal 4, 173–183.
Zhang L, Yang C, Chen S, Wang G, Shi B, Tao X, Zhou L, Zhao J (2017). Long noncoding RNA DANCR is a positive regulator of proliferation and chondrogenic differentiation in human synovium-derived stem cells. DNA Cell Biol 36, 136–142.
Zhu D, Mackenzie NC, Millan JL, Farquharson C, MacRae VE (2011). The appearance and modulation of osteocyte marker expression during calcification of vascular smooth muscle cells. PLoS One 6, e19595.